Version 2/12.7.2012

Generation current temperature scaling

Part-II: Experimental data

Technical Note by A.Chilingarov, Lancaster University

1. Review of published results

Bulk generation current plays an important role in heavily irradiated sensors where it usually dominates in the observed current. In non-irradiated sensors the generation current is typically quite small and can easily be obscured by a current over the physical edge, soft breakdown, etc. Therefore the review below covers only the results obtained with irradiated Si sensors.

The *I(T)* dependence is supposed to be described by

$$I(T) \propto T^2 \exp\left(-\frac{E_{eff}}{2kT}\right). \qquad (1)$$

where T is the absolute temperature and k is the Boltzman constant. Table 1 contains the values of effective energy gap E_{eff} from Refs. [1-8]. For Ref. [5] the only information available is the E_{eff} value.

Some authors use the *I(T)* dependence with T^m in front of the exponential term where $m \neq 2$. As shown in Ref. [9] the E_{eff} measured with such parameterisation, E_e^m, can be at any temperature T converted to an equivalent value of E_{eff} corresponding to m=2:

$$E_{eff}^{eq} = E_{eff}^{m} + 2kT(m-2) \qquad (2)$$

Note that this approximation is valid only for the temperatures around the value of T used in the eq. (2). In Ref. [3] the authors used the parameterisations with m=0 and m=3/2. The E_{eff} found for the latter, 1.34 eV, was corrected to the equivalent E_{eff} for m=2 at typical in their measurements temperature of 293K, that resulted in the value of 1.31 eV shown in Table 1.

In Ref. [10] the parameterisation with m=0 was used for the fits in the temperature interval of 200÷400K and the value E_{eff}=1.30 eV was obtained. Using eq. (2) this result can be converted to an equivalent E_{eff} corresponding to m=2. For example at

T=273K it gives the value of 1.21 eV close to the average value observed in other experiments. However since the parameterisation used in Ref. [10] differs significantly from the one shown in eq. (1) this result is omitted from Table 1.

Table 1. The values of E_{eff} observed with irradiated *n*-type Si sensors

Ref.	**Irradiation made by**	**With E, GeV**	**Maximum fluence, 10^{14}/cm^2**	**E_{eff}, eV**	**In temperature range, ^{o}C**
[1]	p	12	1.7	1.20	-35 ÷ +25
[2]	p	800	1.2	1.276	+2 ÷ +32
[3]	n	~0.001	10	1.31	around +20
[4]	p	0.65	1.25	1.20	-4 ÷ +24
[5]	N/A	N/A	N/A	1.14	N/A
[6]	p	24	3	1.26	-14 ÷ -6
[7]	p	24	3	1.21	-30 ÷ -10
[8]	mostly π[1]	few	0.5[2]	1.13	-24÷+12
			Total average:	**1.216±0.057**	
			Without max and min values:	**1.214±0.049**	

Averaging all results and after excluding the maximum and minimum values gives practically the same answer close to 1.215 eV. The standard deviation is 0.06 eV for the first case and 0.05 eV for the second one.

2. Lancaster results

The results presented in this section were obtained in different studies in Lancaster with irradiated Si sensors. It is worth noting that some studies were not aimed at the investigation of Current-Temperature dependence and therefore were not optimised for this purpose.

[1] particles crossing the VELO system in LHCb detector
[2] 1 MeV neutron equivalent

Usually the I(T) dependence is measured at a fixed bias, typically at or slightly above the full depletion voltage. It is assumed that in this case the current is dominated by the one generated in the bulk. We have investigated the variation of I(T) dependence with bias in a wide voltage range. For bulk generation current the quality of the fit by eq. (1) should remain good and the value of E_{eff} stable independently of bias voltage. Only the data satisfying these requirements were considered as representing the genuine effect. One obvious difficulty in measuring I(T) dependence is the sensor warming above the reference temperature by the power dissipation in it – so called self-heating. It leads to a steady increase of E_{eff} with bias that can be suppressed by a proper choice of the bias values. More detailed discussion of the criteria for the point selection is made in Section 2.4.

Typical data set consisted of several I-V scans made at different temperatures. Then the bias points were combined to form a representative set of groups and in each group the average current was calculated at every temperature. For each bias group the current dependence on temperature was fit by eq. (1). To give equal weight to the points with significantly different absolute values a fixed relative error was assigned to the points and used in the fit.

2.1 **Sensors and their irradiation**

The presented data are for 5 sensors: a) 3 microstrip detectors made of *p*-type material with sensitive area of 1x1 cm^2 , 500 μm thickness and strip pitch of 80 μm and b) 2 diodes made of *n*-type material with sensitive area of 0.5x0.5 cm^2 and 300 μm thickness. The information about the irradiation is presented in Table 2. The quoted fluence is equivalent to that of 1 MeV neutrons.

Table 2. The sensors and their irradiation

Sensor name	**Sensor type**	**Si type**	**Irradiation made by**	**With E, MeV**	**1MeV n equiv. fluence, 10^{14}/cm^2**
x2y4	μ-strip	*p*	p	26	0.1
x4y1	μ-strip	*p*	p	26	1.0
x5y2	μ-strip	*p*	p	26	10
S62	diode	*n*	n	~1	0.82
M41	diode	*n*	n	~1	1.1

Microstrip detectors were irradiated at -40^{o}C and the diodes at room temperature. In all cases the sensors were irradiated without bias. After irradiation the sensors were kept at room temperature for a few days to allow some beneficial annealing. After this the sensors were stored and the measurements with them were made at sub-zero temperature to prevent further annealing. For the same reason rare measurements at temperatures above 0^{o}C were made as brief as possible. Further details about the *p*-type sensors may be found in Ref. [11] and about *n*-type sensors in Ref. [12]. The latter describes also the measurement set-up.

2.2 **Results for the *p*-type sensors**

The I-V dependence was measured with bias voltage applied to the sensor backside, grounded innermost guard ring (GR) and the strip area grounded via an ammeter which gave the current through the central part of the sensor, I_c, used in this study. The bias voltage was always negative. In the text below its absolute value is used. To suppress systematic effects due to possible drift with time the temperature sequence of the I-V scans was non-monotonic. Measurements at the same temperature were made in the beginning and the end of the scan series as a cross-check. The errors used in the I_c vs T fit were set at 1% of the current value.

2.2.1 **Sensor x2y4 irradiated by 10^{13} 1 MeV *n* equivalent fluence**

I-V scans were performed at 9 temperatures in the following sequence: -20^{o}C, -32^{o}C, -24^{o}C, -12^{o}C, -4^{o}C, 0^{o}C, -8^{o}C, -16^{o}C, -28^{o}C, -20^{o}C. The results are shown in Fig.1a.

Around 30 V the I-V curves have a “kink” indicating full depletion of the sensor. Below this voltage the current grows approximately as $(U_{bias})^{1/2}$ (shown by a line in Fig.1) and above it is almost constant. These features indicate the bulk generation as a major source of the current.

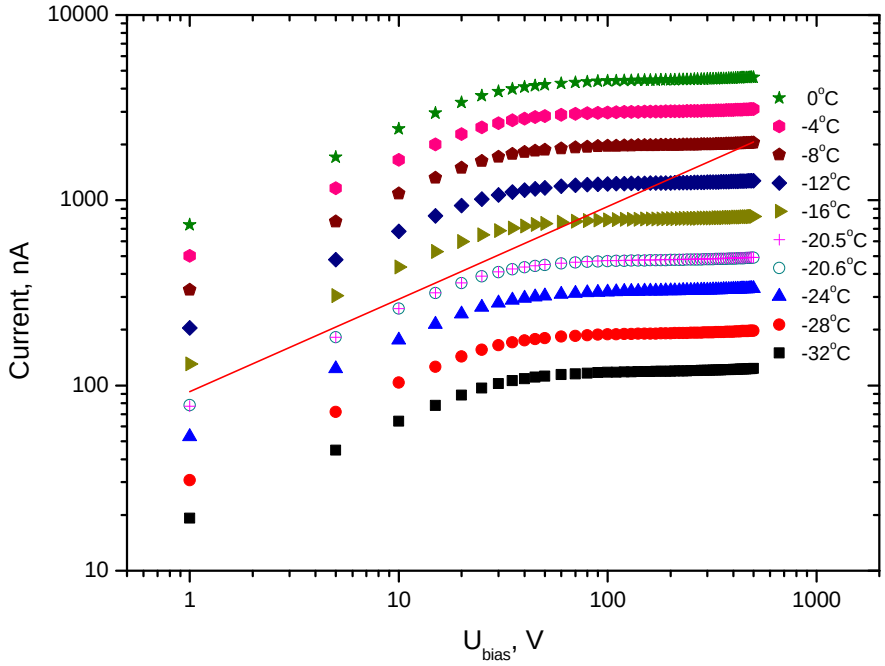

Fig.1a. I_c-V curves for sensor x2y4 irradiated by 10^{13} 1 MeV neutron equivalent fluence. The line shows $(U_{bias})^{1/2}$ dependence.

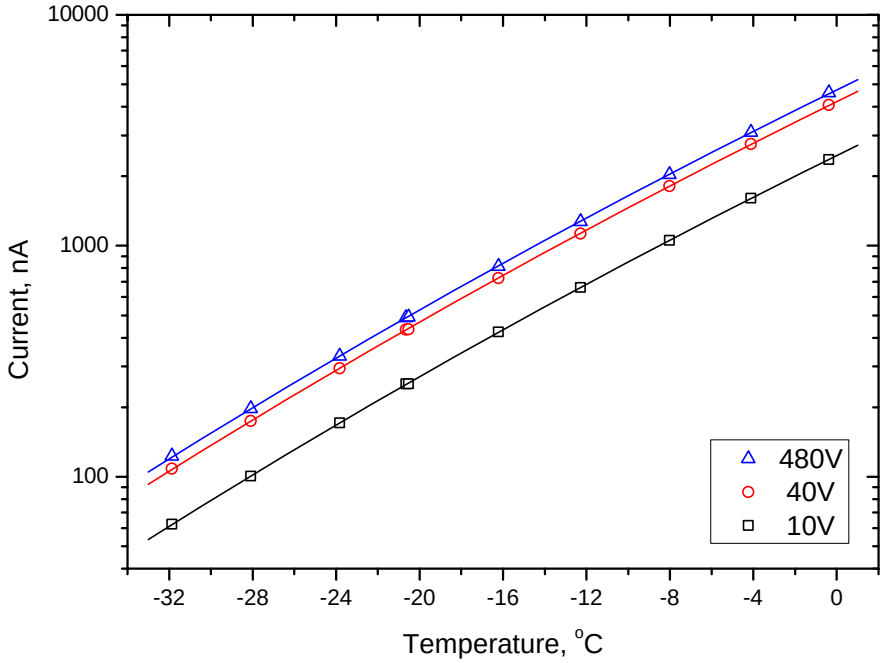

Fig.1b. Average current vs. temperature for 3 bias groups fit by the function (1).

For the analysis 54 bias points from 5 to 490V were combined by 3 in 18 groups and fit as described on p.3. The examples of such fits are shown in Fig.1b. Typical value of χ^2/Ndf was ~0.25 which shows that the spread of the current values around the fit line was about 0.5%.

The E_{eff} values found in the fits are presented in Fig.2 for two temperature intervals: all points (as in Fig.1b) and with two highest temperatures omitted, i.e. from -32°C to -8°C. After relatively sharp decrease at two lowest values further bias dependence of E_{eff} is rather weak. Excluding the first two points (shown in Fig.2 by open symbols) the average E_{eff} value was calculated for both temperature intervals. The average of the obtained two values, 1.2156 eV, was taken as the final result and their sigma, 0.0029 eV, as its standard deviation. These results are also shown in Fig.2.

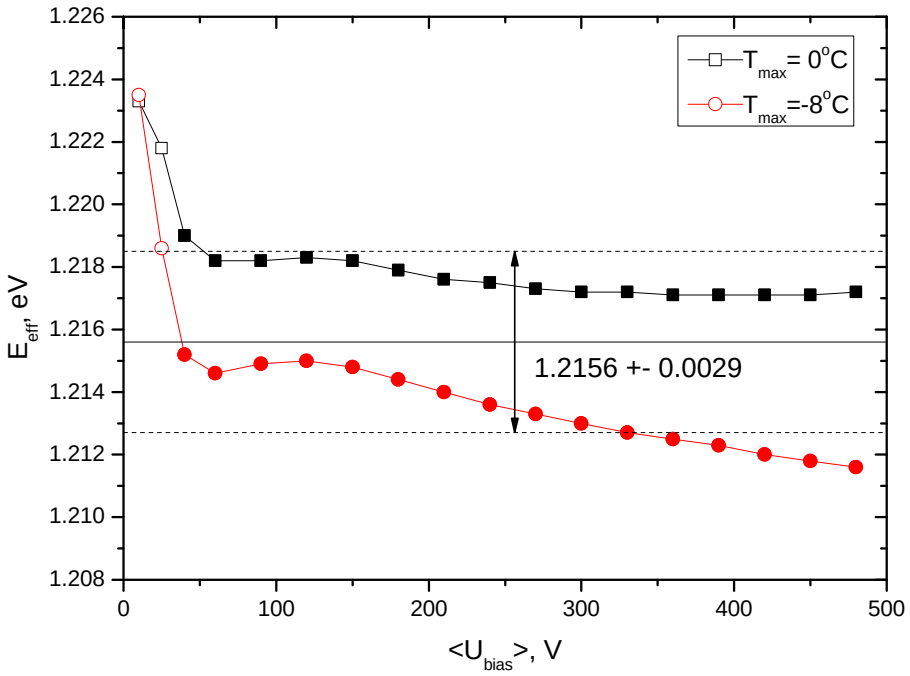

Fig.2. *Eeff* vs. bias for x2y4 sensor in two temperature intervals. The lines are the average and standard deviation calculated for the points shown by the filled symbols.

2.2.2 **Sensor x4y1 irradiated by 10^{14} 1 MeV *n* equivalent fluence**

I-V scans were performed at 8 temperatures in the following sequence: -20°C, -12°C, -16°C, -28°C, -24°C, -31°C, -20°C, -4°C, -8°C. The results are shown in Fig.3. Around

420 V the I-V curves exhibit a “kink” indicating full depletion of the sensor. It is clear at low temperatures but is practically invisible at the highest temperature. Below this voltage the current grows approximately as $(U_{bias})^{1/2}$ (the line in Fig.3) that indicates the bulk generation as a major source of the current at those bias values. Steady increase of the current gradient above the kink with temperature is probably due to the sensor self-heating.

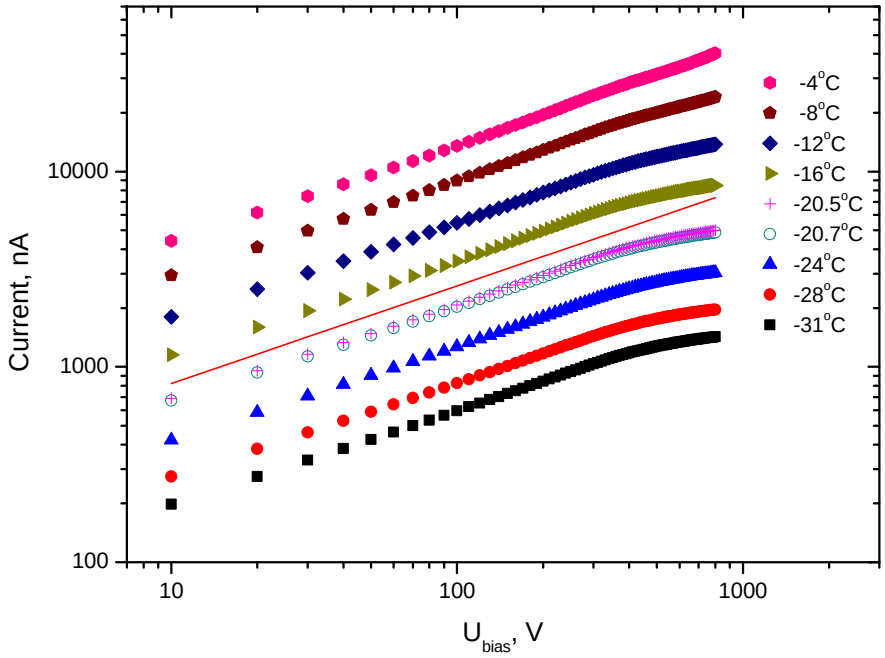

Fig.3. I_c-V curves for sensor x4y1 irradiated by 10^{14} 1 MeV neutron equivalent fluence. The line shows $(U_{bias})^{1/2}$ dependence.

For the analysis 80 bias points from 10 to 800V were grouped by 5 in 16 groups and fit as described above. Typical χ^2/Ndf values found in the fits with 1% errors were <0.5 showing that the actual errors are <0.7%.

The E_{eff} values found in the fits are presented in Fig.4. Each curve corresponds to the maximum temperature of the used interval, T_{max}. The minimum temperature was always -31°C. For T_{max} < -12°C the E_{eff} is about constant up to the bias of ~600V but grows with bias above this value. For higher T_{max} the E_{eff} grows steadily with bias. Such behaviour again indicates the sensor self-heating at high dissipated power. Therefore only the data for T_{max} up to -16°C were used in further analysis. In addition

the points for U_{bias} >600 V were also excluded. Using the remaining points (shown in Fig.4 by the filled symbols) the average E_{eff} was calculated for each of 3 used temperature intervals. The average of the obtained 3 values, 1.219 eV, was taken as the final result and their standard deviation of 0.006 eV as its error. These data are also shown in Fig.4.

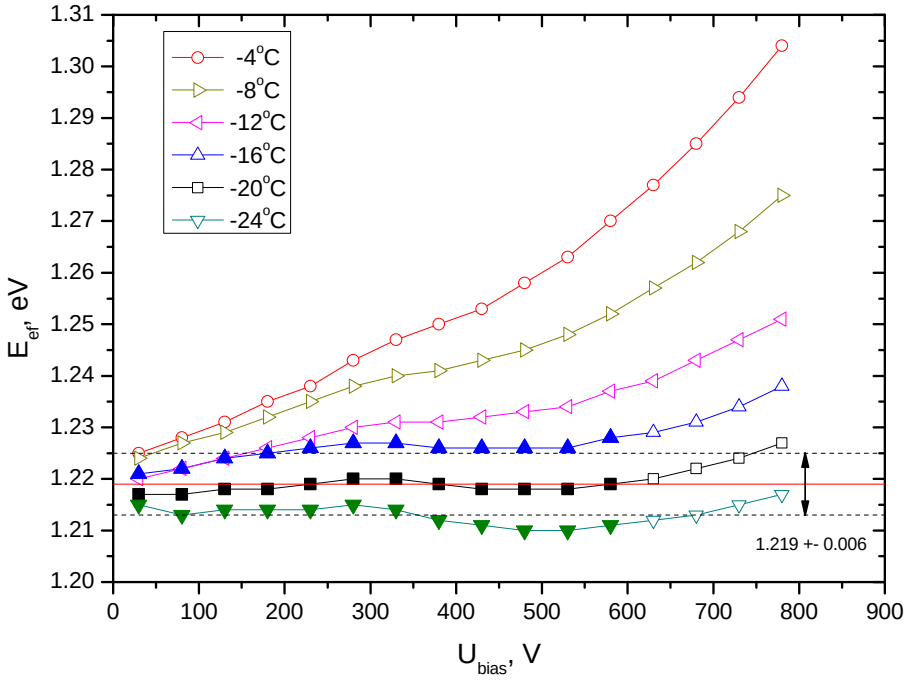

Fig.4. *Eeff* for x4y1 sensor vs. average bias. Each set corresponds to a specific maximum temperature of the used interval. Solid line shows the average value and the dashed lines the standard deviation calculated using the filled points.

2.2.3 **Sensor x5y2 irradiated by 10^{15} 1 MeV *n* equivalent fluence**

I-V scans were performed at 8 temperatures in the following sequence: -32°C, -20°C, -26°C, -30°C, -28°C, -18°C, -22°C, -24°C, -20°C. The results are shown in Fig.5. The currents grow steadily with bias indicating the full depletion voltage above the value of 700 V, maximum used in the scans. At low volts the currents grow approximately as $(U_{bias})^{1/2}$ (shown by the line in Fig.5) that indicates the bulk generation as a major source of the current at those bias values. Steady increase of the current gradients with bias and temperature is probably due to the sensor self-heating.

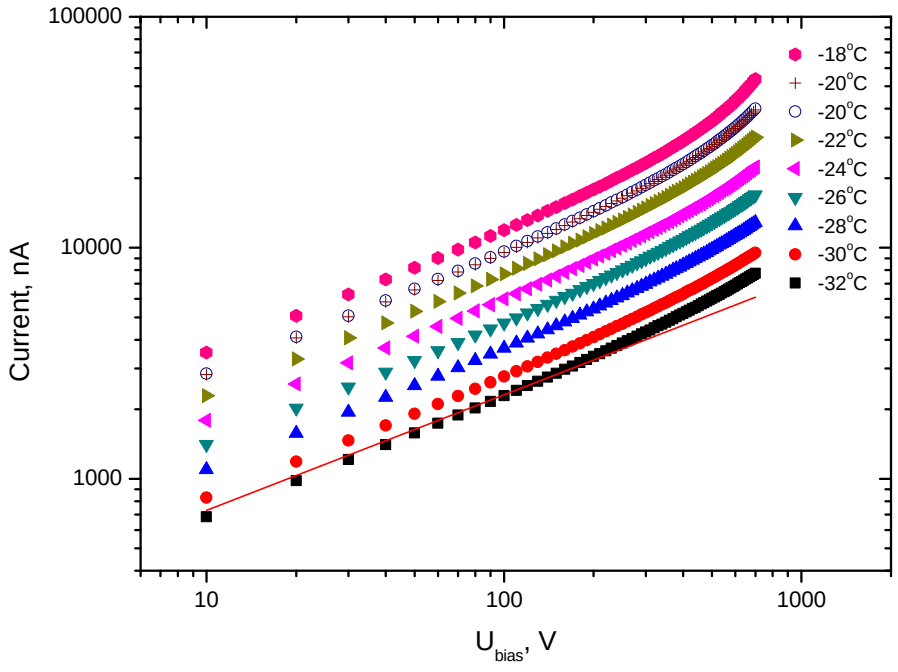

Fig.5. I_c-V curves for sensor x5y2 irradiated by 10^{15} 1 MeV neutron equivalent fluence. The line shows $(U_{bias})^{1/2}$ dependence.

The data fits were made for 18 groups formed by combining 54 bias points from 10 to 540V by 3. Typical χ^2/Ndf values found in the fits with 1% errors were ~0.5 showing that the actual errors are ~0.7%.

The E_{eff} values found in the fits are presented in Fig.6. Each curve corresponds to the maximum temperature of the used interval, T_{max}. The minimum temperature was always -32°C. In all cases the E_{eff} grows steadily with bias. The rate of this growth increases with bias and temperature. Such behaviour is typical for the sensor self-heating due to high dissipated power. To minimise these effects only the data for U_{bias} < 220 V were used. These points are shown in Fig.6 by the filled symbols. The average E_{eff} was calculated for each of 4 used temperature intervals. The average of the obtained 4 values, 1.199 eV, was taken as the final result and their standard deviation of 0.006 eV as its error. These data are also shown in Fig.6.

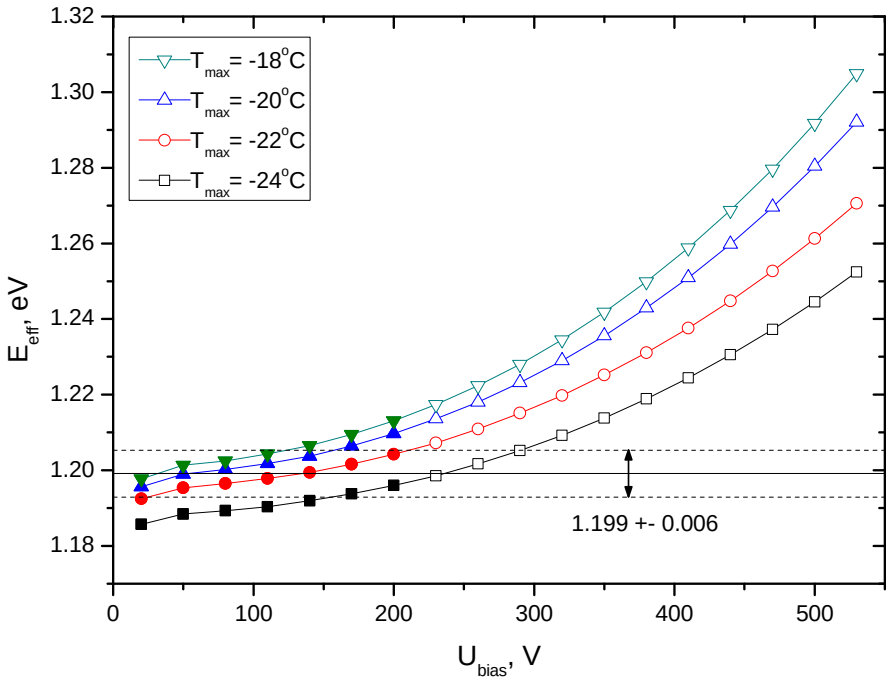

Fig.6. *Eeff* for x5y1 sensor vs. average bias. Each set corresponds to a specific maximum temperature of the used interval. Solid line shows the average value and the dashed lines the standard deviation calculated using the filled points.

2.3 **Results for the *n*-type sensors**

I-V dependence was measured with positive bias voltage applied to the sensor backside, grounded guard ring and the sensitive area grounded via an ammeter, which measured the current through the central part of the diode I_c. The current measurement accuracy in these experiments was lower than for the data presented above. Therefore the errors used in the fits were set at 5%.

2.3.1 **Sensor S62**

The analysed data were collected during the study described in detail in Ref. [12]. The I_c-V measurements were performed simultaneously with C-V measurements, which were the main point of investigation. The temperature sequence was the following: 0°C, -24°C, -12°C, +12°C. Typically 16 bias voltage scans were made at each

temperature. For the present analysis the average I_c-V curve was produced for each temperature. They are shown in Fig.7.

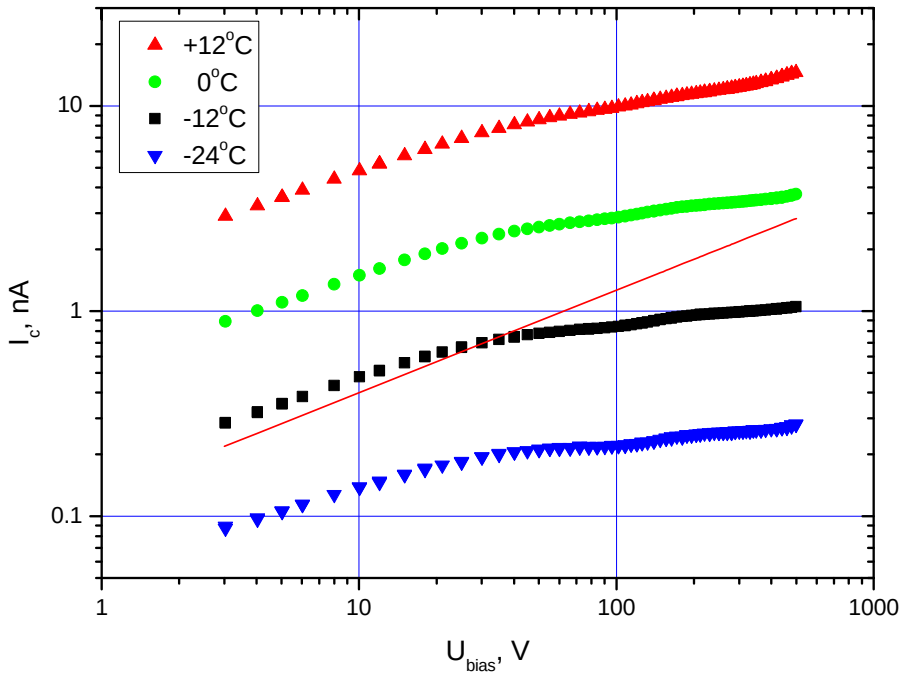

Fig.7. I_c-V curves for sensor S62. Each one is the average of 16 voltage scans. The line shows $(U_{bias})^{1/2}$ dependence.

At ~30 V the curves have a "kink" which is more pronounced at low temperatures but is almost invisible at high temperature. Below this voltage the currents grow as $(U_{bias})^{0.4}$ rather than $(U_{bias})^{0.5}$ (also presented in Fig.7) expected for the current generated in the bulk. This can be due to a contribution from the currents of another type. Above the "kink" the current gradient increases with temperature indicating sensor self-heating at high dissipated power.

The current was measured twice at each bias and thus every curve contains 124 points at 62 bias voltages. Starting from U_{bias}=5V the points (120 in total) were grouped by 10 forming 12 bias groups used for the fits. Typical χ^2/Ndf values of ~0.5 found in the fits show that the assumed 5% errors are close to the actual ones. Fig.8 shows the E_{eff} vs average bias for 12 bias groups.

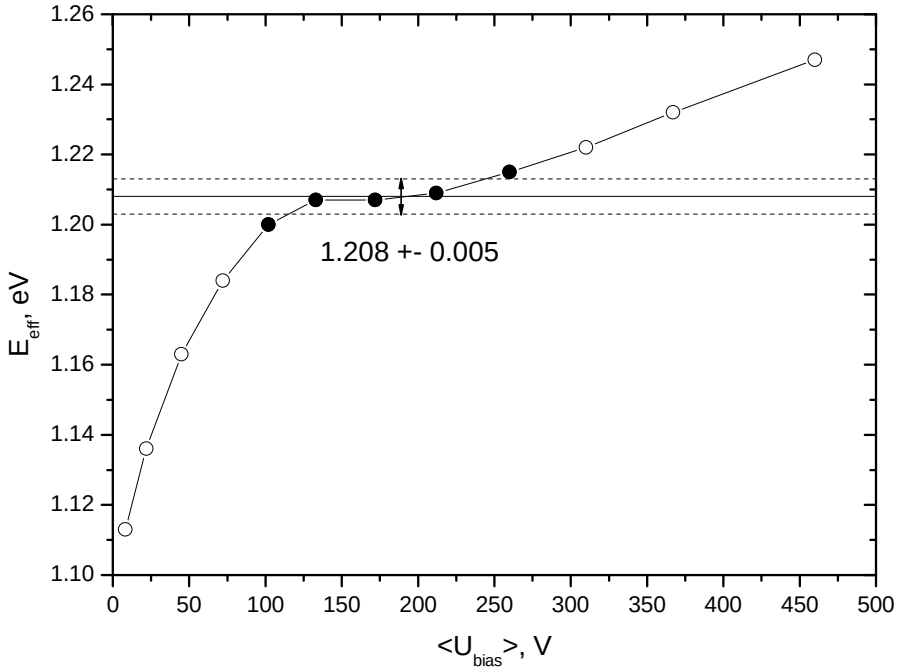

Fig.8. E_{eff} vs average bias for sensor S62. The average value and standard deviation is shown for 5 points marked by filled symbols.

At low voltage the E_{eff} increases steeply with bias. Then it plateaus but above 250 V starts to grow again though with lower gradient. Five points around the plateau region (marked by the filled symbols in Fig.8) have the average value of 1.208 eV and the standard deviation of 0.005 eV. These numbers are also shown in Fig.8.

2.3.2 **Sensor M41**

The data were collected during the study described in detail in Ref. [13]. The I_c-V measurements were performed simultaneously with C-V measurements, which were the main point of investigation. The temperature sequence was the following: 0^oC, -8^oC, -16^oC, $+8^oC$, $+16^oC$, $+25^oC$, $+32^oC$, $+16^oC$ (second time). The second round of measurements at $+16^oC$ showed systematically lower currents than in the first round. This meant that a noticeable annealing happened during the measurements at $+25^oC$, and $+32^oC$. Therefore only the results for the first five temperature series (up to the first $+16^oC$) were analysed here. At each temperature typically 4 bias voltage scans were made. For the present analysis the average I_c-V curve was produced for each temperature. They are shown in Fig.9.

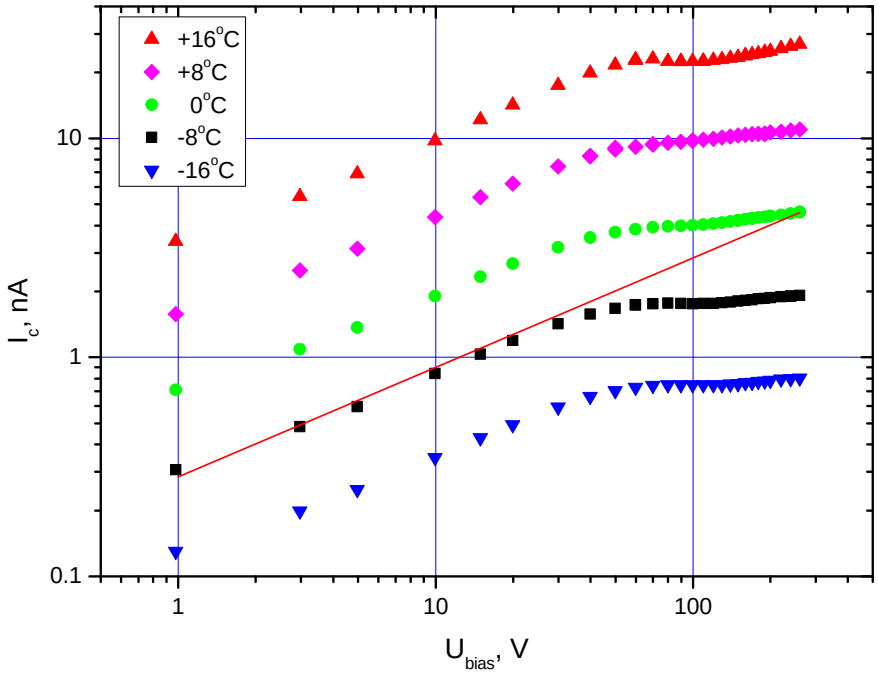

Fig.9. I_c-V curves for sensor M41. Each curve is the average of 3 or 4 voltage scans. The line shows $(U_{bias})^{1/2}$ dependence.

At ~50 V the curves have a "kink" indicating full depletion of the sensor. Below this voltage the currents grow approximately as $(U_{bias})^{0.5}$ shown by the line in Fig.9. Above the "kink" the current is almost constant. This behaviour corresponds to the expectations for the bulk generated current. An increase of the current gradient with temperature at high volts indicates sensor self-heating at high dissipated power.

The current was measured twice at each bias and every curve contains 54 points at 27 bias voltages. Starting from U_{bias}=3V the points (52 in total) were grouped by 6 for the first 36 points and then by 8 for the remaining 16 points thus forming 8 bias groups used for the fits. Typical χ^2/Ndf values of ~0.5 found in the fits show that the assumed errors are close to the actual ones.

Fig.10 shows the E_{eff} vs average bias for 8 bias groups. For the fits made through all 5 temperature points the E_{eff} value steadily grows with bias that is probably due to the sensor self heating. If +16°C points are excluded from the fits the E_{eff} is about

constant in the first 4 points but starts to grow quickly with bias above 100V. The reason for this is probably self-heating again

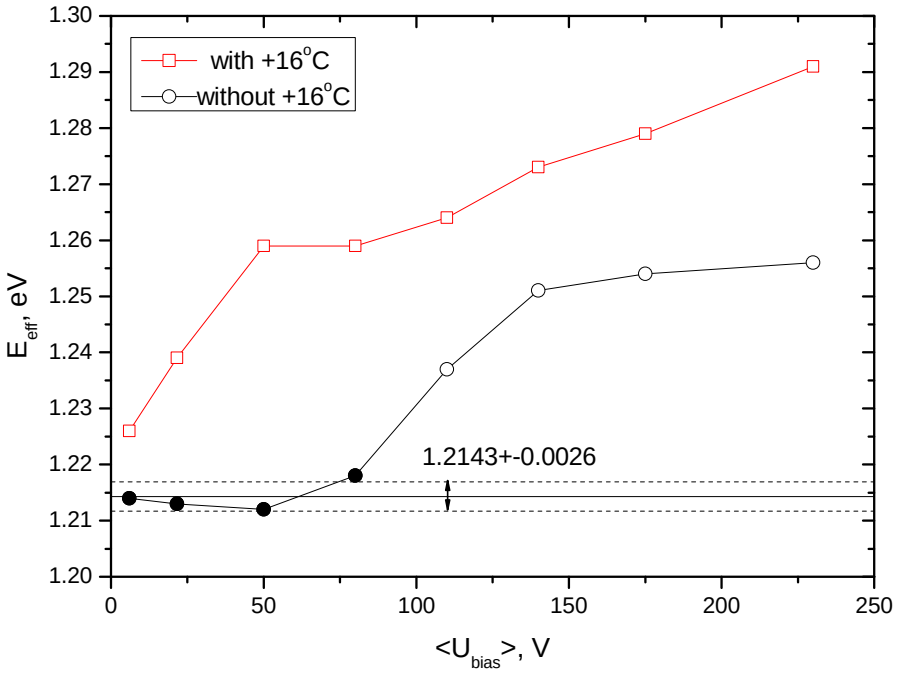

Fig.10. E_{eff} vs average bias for sensor M41 in the fits through all points and without +16°C. The average value and standard deviation is shown for the points marked by the filled symbols.

The average value of the first 4 points for the fits without +16°C is 1.2143 eV and their standard deviation is 0.0026 eV. These numbers are also shown in Fig.10.

2.4 **Discussion**

In the investigation of the current-temperature dependence care should be taken in selecting the results corresponding to the bulk generation current and avoiding the effects of sensor self-heating. The latter usually manifests itself as a steady increase of the parameter E_{eff} with bias. Four out of five sensors analysed here showed this effect and some temperature or bias points (and sometimes both) had to be excluded on this ground from the final results. For the sensor irradiated by 10^{15} neq/cm^2 the self-heating effects could not be avoided but only minimised.

For genuine generation current E_{eff} should not depend on bias. When this is not the case (after the self-heating is eliminated) it is possible that the measured current has a significant contribution from the other types of the current. On this ground several low bias points were excluded from the final result for the sensors x2y4 and S62. It is worth noting that for the latter the current growth with bias below depletion differs from the expected $(U)^{1/2}$ dependence that is also an indication of another current type contribution. For the sensor irradiated by 10^{15} neq/cm^2 the slope of the log(I)-log(V) curve increases steadily with bias. Even at the low volts it is higher than expected value of 0.5. This can be due either to the self-heating or to more complicated dependence of the depleted thickness with bias in so heavily irradiated sensors. Note that for this sensor all measurements are made well below the full depletion voltage. Final results are summarised in Table 3.

Table 3. Summary of the results

Sensor name	**IV"kink" at, V**	**lnI-lnU slope**	**Bias range used, V**	**Temperature range used, ^{0}C**	**Eeff, eV**	**Standard deviation, eV**
x2y4	29	0.49	35-490	-32 ÷ 0	1.2156	0.0029
x4y1	420	0.49	10-600	-31 ÷ -16	1.2188	0.0063
x5y2	N/A	0.52*	10-210	-32 ÷ -18	1.1991	0.0062
S62	32	0.40	90-280	-24 ÷ +12	1.2076	0.0054
M41	50	0.48	3-90	-16 ÷ +8	1.2143	0.0026
				Average:	**1.211**	**0.008**

Second column shows the voltage at which the "kink" indicating full depletion is observed in log(I_c)-log(V) plot and the third column the slope in this plot below the "kink". The fourth and fifth columns show the bias and temperature ranges used in the final result, which is presented in the last two columns. Averaging the E_{eff} values from column 6 with equal weight (i.e. ignoring the errors from column 7) gives 1.211 eV with a standard deviation of 0.008 eV. This information is presented graphically in Fig.11. As can be seen from this plot all results are consistent within their relatively

* For the bias range 10÷100 V.

small uncertainties despite significant difference in sensors, irradiations and measurement procedures. Absence of the analysis of a possible E_{eff} dependence on bias voltage and temperature range in publications reviewed in Section 1 may be responsible for a relatively large spread of the results.

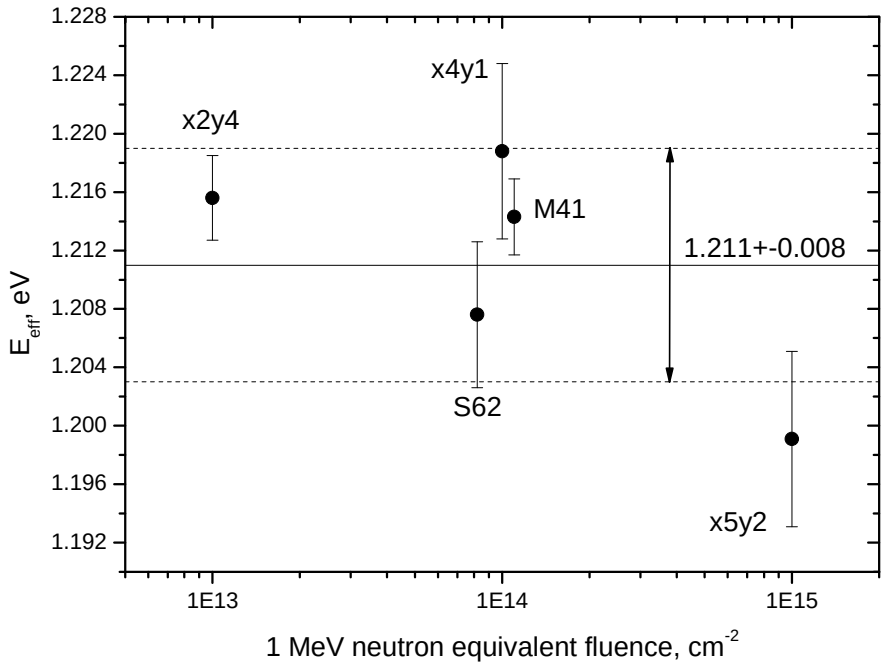

Fig.11. E_{eff} for individual sensors vs 1 MeV neutron equivalent fluence. The overall average and the standard deviation are shown by the lines.

3. Conclusions

Within uncertainties the experimental E_{eff} values for all sensors investigated in Lancaster agree with the expected value of 1.21 eV obtained for temperature range of ±30°C as explained in the first part of this Note [9]. The average E_{eff} value of Lancaster measurement is 1.211 eV and the standard deviation of the individual sensor results is 0.008 eV. For the reviewed published results the average is 1.215 eV with the standard deviation of the individual entries of 0.05 eV for the data excluding minimum and maximum values and of 0.06 eV for all data.

References

1. T.Ohsugi et al., NIM A265 (1988) 105.
2. M.Nakamura et al., NIM A270 (1988) 42.
3. K.Gill et al., NIM A322 (1992) 177.
4. E.Barberis et al., NIM A326 (1993) 373.
5. H.Feick, PhD Thesis, DESY F35D-97-08, 1997, Table E.6. No information on the studied sensors and their irradiation is available.
6. L.Andricek et al., NIM A436 (1999) 262.
7. ATLAS SCT Barrel Module Final Design Review, SCT-BM-FDR-7, 2002, p.19. The quoted result is $E_{eff}/2k$ = 7019K which gives E_{eff} =1.210 eV.
8. A.Hickling et al., Technical Note CERN-LHCb-PUB-2011-021, December 30, 2011.
9. A.Chilingarov, "Generation current temperature scaling", 9.5.2011, Technical Note RD50-2011-01 available at: http://rd50.web.cern.ch/rd50/doc/Internal/rd50_2011_001-I-T_scaling.pdf
10. E.Verbitskaya et al., "Temperature dependence of reverse current of irradiated Si detectors", Talk at the 20th RD50 Workshop, Bari, May 30 – June 1, 2012. Available at: https://indico.cern.ch/getFile.py/access?contribId=1&sessionId=1&resId=1&materialId=slides&confId=175330
11. L.Eklund et al., NIM A623 (2010) 162.
12. D.Campbell, A.Chilingarov, T.Sloan, NIM A492 (2002) 402.
13. L.J.Beattie, PhD Thesis, RAL-TH-1998-015, 1998.